Imitation Learning Control for Thermoacoustic Stabilization of a Rijke Tube

Gustavo Artur de Andrade, Mirko Fiacchini, Christophe Prieur

Imitation learning control for thermoacoustic stabilization of a Rijke tube*

Gustavo Artur de Andrade[1], Mirko Fiacchini[2] and Christophe Prieur[2]

***Abstract*— This work studies the use of Neural Network (NN) boundary controllers to stabilize thermoacoustic instabilities in a Rijke tube. The dynamics of this phenomenon are governed by a system of 4×4 hyperbolic linear partial differential equations (PDEs) for the acoustic wave propagation, plus a linear ordinary differential equation (ODE) for the heat release. The control action is applied in one of the left boundary conditions, characterizing this system as underactuated. Previous results in the literature showed that this control problem can be solved by the backstepping methodology with stability guarantees in the $\mathcal{L}_2$ sense. However, the stabilization and closed-loop system performance are usually affected by uncertainties. To tackle this issue, we rewrite this PDE-ODE boundary control problem as an imitation learning problem for stabilizing the system by observing the state values of a numerical simulator of the Rijke tube system under different operating conditions. Additionally, we present a Lyapunov-based method with local sector quadratic constraints to analyze the stability of the closed-loop system with the NN controllers. We demonstrate by simulations that the NN controller is able to stabilize the system under uncertain conditions, with the potential to overcome the performance of the backstepping.**

I. INTRODUCTION

Modern turbine technologies rely on lean premixed combustion to comply with low-emission standards. The main challenge of these processes is the increased likelihood of high-amplitude pressure fluctuations, commonly referred to as thermoacoustic instability, due to the positive feedback loop between the acoustic modes and the fluctuating heat release from the combustion chamber. At best, the consequences of these instabilities are increased noise, and reduced system performance and durability. At their worst, the oscillations highly increase the average pressure, resulting even in the damage of the system. Therefore, the capability to predict and control thermoacoustic oscillations is of utmost importance for further advances in combustion technologies.

Much of the early work on the mitigation of these instabilities focused on developing passive methods to dampen the oscillations by ad-hoc physical augmentation of the system [1]. However, these methodologies work well only on a given operating region and can be incredibly expensive. Recent results in the area have shown that active control is an alternative technology able to reduce oscillations over a wide range of conditions in order to achieve the desired performance.

Traditionally, the Rijke tube has been used as a benchmark system to study control strategies to mitigate thermoacoustic instabilities. This system was discovered in the 1850s by P. L. Rijke [5] and consists of a vertical tube open at both ends with an embedded heat source. The air that traverses the heating zone expands, causing the local pressure to increase. The pressure acoustically propagates along the tube and returns (due to the boundary conditions), inducing a feedback loop: the pressure at the current time is affected by itself at earlier time instants, leading to time-delayed dynamics in the thermoacoustic coupling. Thus, a hyperbolic partial differential equation (PDE) system for the acoustic dynamics plus an ordinary differential equation (ODE), describing the heat release dynamics, is suitable to mathematically represent this system [4]. A speaker placed under the tube is generally used as an actuator to suppress the oscillations, which yields a boundary control problem.

Over the past fifty years several researchers developed control strategies based on reduced phenomenological models, as can be seen in [8]. More recently, control strategies based on the PDE model of thermoacoustic instabilities have been proposed in the literature, such as the backstepping controller proposed in [3] or the delayed control laws developed in [7]. A disadvantage of these model-based control strategies is that they require knowledge of the acoustic and thermodynamic parameters to characterize the system dynamics. Usually, their values must be estimated through correlation analysis with other variables or obtained by calibrating the model with real sensor data through an involved validation process that works on specific conditions. To reduce the need for modeling, a data-driven controller that requires minimal modeling information is desirable. This challenge can be addressed by the use of neural network (NN) controllers.

In the last years, neural networks (NN) have drawn attention from the control community since they have the strength to map input-output relationships with only a priori input-output information. In this case, NNs can be used as parametric approximators for functions of states whose weights are updated automatically to learn the control law and, consequently, circumvent the model complexity and identification process faced by model-based controllers. In addition, NN controllers can deal with stochastic conditions by considering random events in their training process, whereas model-based control approaches for PDE systems still face challenges in tackling uncertainties [2].

*This work was partially supported by CAPES under the grant 88887.522001/2020-00 (C-CAIT, SticAmSud), and MIAI@Grenoble Alpes (ANR-19-P3IA-0003).

[1]Gustavo Artur de Andrade is with Department of Automation and Systems, Universidade Federal de Santa Catarina, 88040-900, Florianópolis, SC, Brazil. E-mail: gustavo.artur@ufsc.br

[2]Mirko Fiacchini and Christophe Prieur are with Université Grenoble Alpes, CNRS, Grenoble-INP, GIPSA-lab, F-38000, Grenoble, France. E-mails: mirko.fiacchini@grenoble-inp.fr, christophe.prieur@gipsa-lab.fr

In this work, we propose a state feedback NN controller that imitates the backstepping control law proposed in [3], i.e. behavior cloning where the dataset is taken from the expert. Importantly, the proposal does not require any prior knowledge of the model structure, or model calibration. Instead, the control input is obtained by a training process with a simulator of the system. Thus, minimal assumptions on the infinite-dimensional control problem yet obtain good controllers through a data-driven process. Additionally, a stability analysis of the NN controllers is presented by using sector conditions to represent the nonlinear activation functions. The advantage of this framework is that all the classic results of robust control theory became available to access the asymptotic stability condition of the zero equilibrium of the closed-loop system. We demonstrate by simulations that the NN controller is able to stabilize the system under uncertain conditions, with the potential to overcome the performance of the backstepping controllers.

The outline of this article is as follows. Section II summarizes the Rijke tube model. The backstepping controller is briefly presented in Section III. Section IV details the imitation learning approach for boundary control of the Rijke tube model. Section V includes the numerical results, comparing the closed-loop performance of the system with the backstepping controller in different scenarios. Finally, Section VI summarizes the main results and discusses future works.

II. PROBLEM UNDER CONSIDERATION

The Rijke tube model used in this work is inspired by the one described in [3], which is given by the following set of linear PDEs-ODE in the so-called characteristic coordinates:

$$\partial_t \alpha(t,z) + \Lambda \partial_z \alpha(t,z) = 0, \tag{1}$$

$$\partial_t \beta(t,z) - \Lambda \partial_z \beta(t,z) = 0, \tag{2}$$

$$\tau_{hr}\dot{Q}(t) + Q(t) = c_2(\alpha_1(t,1) - \alpha_2(t,1)), \tag{3}$$

where

$$\alpha = (\alpha_1, \alpha_2), \quad \beta = (\beta_1, \beta_2), \quad \Lambda = \operatorname{diag}\{\lambda_1, \lambda_2\}.$$

The boundary conditions are given by

$$\alpha(t,0) = N_i \beta(t,0) + N_u U(t), \tag{4}$$

$$\beta(t,1) = N_f \alpha(t,1) + N_q Q(t), \tag{5}$$

with

$$N_i = \begin{pmatrix} k_0 & 0 \\ 0 & 1 \end{pmatrix}, \quad N_u = \begin{pmatrix} 2 \\ 0 \end{pmatrix},$$
$$N_f = \begin{pmatrix} 1 & 0 \\ 0 & k_L \end{pmatrix}, \quad N_q = \begin{pmatrix} c_1 \\ c_1 \end{pmatrix}.$$

In (1)-(5), the time t belongs to $[0, \infty)$, the space variable z belongs to $[0,1]$, and the characteristic speeds λ_1 and λ_2 satisfies $\lambda_1 > \lambda_2 > 0$. The constants τ_{hr}, c_1 and c_2 are strictly positives, and the reflection coefficients k_L and k_0 belong to $(-1, 0)$. For $i \in \{1, 2\}$, the initial conditions of (1)-(2) are denoted by $\alpha_{i,0}$, $\beta_{i,0}$, and Q_0. They belong to $(\mathcal{L}_2([0,1]))^4 \times \mathbb{R}$.

A. Control Problem

The control problem of the Rijke tube system is to design a feedback control law U such that the zero equilibrium point of (1)-(5) is exponentially stable in the $(\mathcal{L}_2([0,1]))^4 \times \mathbb{R}$ sense. In this work, this control problem will be solved by developing a NN based controller that mimics the backstepping methodology designed in [3]. In this work, we will assume that the values of the states on the entire domain are available for the controller because a scenario with output measurements would require the use of a state observer and an involved training procedure with a large amount of data which still needs to be investigated.

III. BACKSTEPPING CONTROLLER

The backstepping controller for (1)-(5) was first developed in [3] and uses a full-state-feedback control law to stabilize the system. The key idea of this methodology is to find an invertible transformation (the backstepping transformation) so that the transformed states of the system verifies a PDE with the desired stability properties. This transformation also allows finding the control variable in the form of feedback. In the particular case of the Rijke tube system, the kernels of the transformation can be found explicitly, allowing in turn to derive the explicit expression of the control law gains.

The boundary full-state-feedback backstepping controller is given by

$$U_{bs}(t) = \frac{1}{2}\Big(\beta_1(t,0) + \varphi(0)Q(t) + \int_0^1 \alpha_1(t,\xi)K(0,\xi)d\xi + \int_0^1 \alpha_2(t,\xi)G(0,\xi)d\xi + \int_0^1 \beta_2(t,\xi)H(0,\xi)d\xi\Big), \tag{6}$$

where

$$K(z,\xi) = \frac{c_2}{\lambda_1 \tau}\varphi(z-\xi+1) + \frac{\lambda_2}{\lambda_1}H(z-\xi+1,1),$$

$$G(z,\xi) = \begin{cases} 0 & \xi - 1 \le \frac{\lambda_2}{\lambda_1}(z-1), \\ \frac{-c_2}{\lambda_2 \tau}\varphi\left(g_1(z,\xi)\right), & \text{otherwise}, \end{cases}$$

$$H(z,\xi) = \begin{cases} 0 & \xi + 1 \ge \frac{\lambda_2}{\lambda_1}(1-z), \\ \frac{-\alpha c_2}{\lambda_2 \tau}\varphi\left(g_2(z,\xi)\right), & \text{otherwise}, \end{cases}$$

$$\varphi(z) = -c_1 \mathrm{e}^{\frac{z-1}{\lambda_1 \tau}},$$

with $g_1(z,\xi) = z - \frac{\lambda_1}{\lambda_2}(\xi - 1)$ and $g_2(z,\xi) = z + \frac{\lambda_1}{\lambda_2}(\xi + 1)$.

As stated in the next theorem, the control law (6) guarantees the convergence of (1)-(5) in the $(\mathcal{L}_2([0,1]))^4 \times \mathbb{R}$ sense [3].

Theorem 3.1: Consider the system (1)-(5) with the control law (6). Then for any initial condition $\alpha_{i,0}$ and $\beta_{i,0}$, for $i \in \{1,2\}$, in $(\mathcal{L}^2([0,1]))^4$ and $Q_0 \in \mathbb{R}$, the zero equilibrium is exponentially stable in the $(\mathcal{L}_2)^4 \times \mathbb{R}$ sense.

IV. IMITATION LEARNING

In this section, we present the imitation learning (IL) approach for boundary control of the Rijke tube system (1)-(5). Although explicit knowledge of the PDE model is not required, the stability certification analysis of the NN structure, which is based on the framework proposed in [6], is

developed considering the Lyapunov theory for discrete finite dimensional dynamic systems. Thus, as a first step in the IL methodology, the Rijke tube model (1)-(5) is discretized in time and space so that a finite dimension approximate representation can be obtained.

A. Discrete time-space approximation and finite state space representation of the system

We consider a discretized approximation of model (1)-(5) using a Euler scheme in time and space. In this context, the solution of the states α and β are approximated by piecewise constant functions on the discretized spatial and temporal domains $[0,1] \times [0,T]$, with $T > 0$.

Let $\Delta z = 1/(S-1)$ be the length of the spatial discretization, where S is the number of nodes, such that $z_j = (j-1)\Delta z$, $j \in \{1, \ldots, S\}$, are the grid points with

$$0 = z_1 < z_2 < \cdots < z_{S-1} < z_S = 1.$$

Then, the spatial derivatives in (1)-(2) at a given time instant $t \in [0,T]$ and at a given $z \in (0,1)$ can be approximated by $\frac{\partial \alpha_i}{\partial z}(t,z) \approx \frac{\alpha_i(t,z_{j+1}) - \alpha_i(t,z_j)}{\Delta z}$, and $\frac{\partial \beta_i}{\partial z}(t,z) \approx \frac{\beta_i(t,z_{j+1}) - \beta_i(t,z_j)}{\Delta z}$, for $j \in \{1, \ldots, S\}$.

Regarding the time derivative, M constant values are considered over the time horizon $t \in [0,T]$, such that the length of the time discretization is $\Delta t = T/(M-1)$ and the temporal grid points are

$$0 = t_1 < t_2 < \cdots < t_{M-1} < t_M = T,$$

with $t_k = (k-1)\Delta t$, $k \in \{1, \ldots, M\}$.

Then, at a given value of $z \in (0,1)$ and at a given $t \in (0,T)$ the corresponding time derivative approximations are given by $\frac{\partial \alpha_i}{\partial t}(t,z) \approx \frac{\alpha_i(t_{k+1},z) - \alpha_i(t_k,z)}{\Delta t}$, $\frac{\partial \beta_i}{\partial t}(t,z) \approx \frac{\beta_i(t_{k+1},z) - \beta_i(t_k,z)}{\Delta t}$, and $\frac{dQ}{dt}(t) \approx \frac{Q(t_{k+1}) - Q(t_k)}{\Delta t}$.

Using the time and spatial derivative approximations, the model (1)-(5) is transformed into discrete algebraic expressions. More precisely, define the following discrete-time state variables:

$$\begin{aligned} \alpha_{1,j}(k) &= \alpha_1(t_k, z_j), & \beta_{1,j}(k) &= \beta_1(t_k, z_j), \\ \alpha_{2,j}(k) &= \alpha_2(t_k, z_j), & \beta_{2,j}(k) &= \beta_2(t_k, z_j), \\ Q(k) &= Q(t_k), \end{aligned}$$

with $k \in \{1, \ldots, M\}$ and $j \in \{1, \ldots, S\}$. Stacking these variables into the state vector $\zeta \in \mathbb{R}^{n_G}$, with $n_G = 4S + 1$, and using (1)-(5), it is possible to obtain the following compact finite dimensional discrete-time approximation of the Rijke tube system:

$$\zeta(k+1) = A_G \zeta(k) + B_G U(k), \tag{7}$$

where $A_G \in \mathbb{R}^{n_G \times n_G}$, $B_G \in \mathbb{R}^{n_G}$. The explicit expressions of A_G and B_G are omitted in this paper due to lack of space.

Given a state feedback controller, the vector $\zeta^* \in \mathbb{R}^{n_G}$ is an equilibrium point of (7) if and only if

$$(A_G - I)\zeta^* + B_G U^* = 0. \tag{8}$$

Thus, given state and control data pairs from the backstepping methodology described in Section III, our goal is to learn a NN controller from the data to reproduce the demonstrated behavior, while guaranteeing the stability of the zero equilibrium point defined by the solution of (8).

B. Neural network controller

In this work, the NN controller $\pi : \mathbb{R}^{n_G} \to \mathbb{R}$ is assumed to be an ℓ-layer *feedforward neural network* defined as

$$\omega_0(k) = \zeta(k), \tag{9}$$

$$\omega_i(k) = \phi_i(W_i \omega_{i-1}(k) + b_i), \qquad i \in \{1, \ldots, \ell\}, \tag{10}$$

$$U(k) = W_{\ell+1} \omega_\ell(k) + b_{\ell+1}, \tag{11}$$

where $\omega_0 \in \mathbb{R}^{n_0}$ is the input to the network (system states), with $n_0 = n_G$, and for $i \in \{1, \ldots, \ell\}$, $\omega_i \in \mathbb{R}^{n_i}$ is the output from the i-th layer. The operations for each layer are defined by a weight matrix $W_i \in \mathbb{R}^{n_i} \times \mathbb{R}^{n_{i-1}}$, a bias vector $b_i \in \mathbb{R}^{n_i}$, and an activation function $\phi_i : \mathbb{R}^{n_i} \to \mathbb{R}^{n_i}$, which is applied element-wise, that is,

$$\phi_i(\nu) \triangleq \begin{pmatrix} \varphi(\nu_1) & \ldots & \varphi(\nu_{n_i}) \end{pmatrix},$$

where $\varphi : \mathbb{R} \to \mathbb{R}$ is the predefined scalar hyperbolic tangent activation function[1].

In this work, the gradient descent technique is used as the optimization algorithm to minimize the least-square loss function taking into account the error between the learned policy and the expert behavior in order to find a set of weights that best map the states into the desired control signal. In the first step, closed loop data with different initial conditions are generated with the *late-lumping* approximation of the backstepping controller presented in Section III. Then, these data are properly treated for their application into the training process of the NN controller.

Besides the design of the NN controller (9)-(11), we present in the next section a framework, based on [6], to analyze the closed-loop of system (7) under the control law (9)-(11). The idea of this methodology is to extract the bounds of the activation functions once the NNs are trained, and then, develop LMI conditions for the abstracted formulation.

C. Isolation of NN nonlinearities

For $i \in \{1, \ldots, \ell\}$, let $\nu_i \in \mathbb{R}^{n_i}$ be the input to the activation function ϕ_i, that is,

$$\nu_i(k) = W_i \omega_{i-1}(k) + b_i, \quad i \in \{1, \ldots, \ell\}.$$

Then, the operation of the i-th layer can be expressed as $\omega_i(k) = \phi_i(\nu_i(k))$. Gathering the inputs and outputs of all activation functions, we get

$$\nu_\phi \triangleq \begin{pmatrix} \nu_1 \\ \vdots \\ \nu_\ell \end{pmatrix} \in \mathbb{R}^{n_\phi}, \qquad \text{and} \qquad \omega_\phi \triangleq \begin{pmatrix} \omega_1 \\ \vdots \\ \omega_\ell \end{pmatrix} \in \mathbb{R}^{n_\phi},$$

where $n_\phi \triangleq \sum_{i=1}^{\ell} n_i$.

[1]Other activation functions such as sigmoid, rectified linear unit (ReLU), and leaky ReLU, could be used without loss of generality.

Now, define the vector of stacked activation functions $\phi : \mathbb{R}^{n_\phi} \to \mathbb{R}^{n_\phi}$ such that

$$\phi(\nu_\phi) \triangleq \begin{pmatrix} \phi_1(\nu_1) \\ \vdots \\ \phi_\ell(\nu_\ell) \end{pmatrix}. \tag{12}$$

In this framework, the NN control policy π can be rewritten as

$$\begin{pmatrix} U(k) \\ \nu_\phi(k) \end{pmatrix} = N \begin{pmatrix} \zeta(k) \\ \omega_\phi(k) \\ 1 \end{pmatrix}, \tag{13}$$

$$\omega_\phi = \phi(\nu_\phi(k)), \tag{14}$$

where

$$N = \left(\begin{array}{c|cccc|c} 0 & 0 & 0 & \dots & W_{\ell+1} & b_{\ell+1} \\ \hline W_1 & 0 & \dots & 0 & 0 & b_1 \\ 0 & W_2 & \dots & 0 & 0 & b_2 \\ \vdots & \vdots & \ddots & \vdots & \vdots & \vdots \\ 0 & 0 & \dots & W_\ell & 0 & b_\ell \end{array}\right) = \begin{pmatrix} N_{U\zeta} & N_{U\omega} & N_{Ub} \\ N_{\nu\zeta} & N_{\nu\omega} & N_{\nu b} \end{pmatrix}$$

The decomposition (13)-(14) isolates the activation function nonlinearities which in turn allows us to analyze the stability of the controlled system by applying quadratic constraints (QC) that bound the activation functions in a similar fashion as in robust control theory.

D. Quadratic constraints

The key idea of applying QC is to obtain a new representation of the NN controller (13)-(14) where the nonlinear activation functions are substituted by the constraints they impose on the pre- and post- activation signal. Obviously, any property that can be guaranteed in this framework is also satisfied by the original NN as well. A typical QC is the *local sector condition*, which allows us to obtain tight bounds on the graph of the activation functions.

In the scalar case, we say that a nonlinear function $\varphi : \mathbb{R} \to \mathbb{R}$, with $\varphi(0) = 0$, is sector bounded in the sector $[m, r]$, with $m \leq r < \infty$, if the following condition holds for all $\nu \in \mathbb{R}$:

$$(\varphi(\nu) - m\nu)(\varphi(\nu) - r\nu) \leq 0. \tag{15}$$

This concept can be extended to the vectorial case of nonlinear functions, as the one in (12). Indeed, for $i \in \{1, \dots, n_\phi\}$, assume that the i-th activation function ϕ_i in ϕ is sector bounded by $[m_i, r_i]$. Then, it is possible to stack these sectors into vectors $m_\phi, r_\phi \in \mathbb{R}^{n_\phi}$ so that the following condition is satisfied for ϕ:

$$(\phi(\zeta) - M_\phi\zeta)^T(\phi(\zeta) - R_\phi\zeta) \leq 0, \tag{16}$$

with $M_\phi = \text{diag}(m_\phi)$ and $R_\phi = \text{diag}(r_\phi)$.

From (16), it readily follows that

$$\begin{pmatrix} \nu_\phi \\ w_\phi \end{pmatrix}^T \begin{pmatrix} -2M_\phi R_\phi & (M_\phi + R_\phi) \\ (M_\phi + R_\phi) & -2I_{n_\phi} \end{pmatrix} \begin{pmatrix} \nu_\phi \\ w_\phi \end{pmatrix} \geq 0. \tag{17}$$

For the NN controller (13)-(14) the local sector conditions can be obtained by a numerical procedure given the set of weighting matrices, W_i, the bias vectors, b_i, and monotonically non-decreasing activation functions, ϕ_i. Additionally, we will assume an *artificial set of states constraints*, Z, in order to allow us to apply the local sectors. This set is defined by

$$Z = \{\xi \in \mathbb{R}^{n_G} : -h \leq H\xi \leq h,\, h \geq 0\},$$

where $H \in \mathbb{R}^{n_z \times n_G}$ and $h \in \mathbb{R}^{n_z}$.

First, note that the smallest hypercube that bounds the state constraint set Z is $\underline{\zeta} \leq \zeta \leq \overline{\zeta}$, with $\underline{\zeta}, \overline{\zeta} \in \mathbb{R}^{n_G}$. Then, from (9) it follows that ω_0 is bounded below by $\underline{\omega}_0 = \underline{\zeta}$ and above by $\overline{\omega}_0 = \overline{\zeta}$. Now, define $\overline{n} = \frac{1}{2}(\overline{\omega}_0 + \underline{\omega}_0)$, $\underline{n} = \frac{1}{2}(\overline{\omega}_0 - \underline{\omega}_0)$, and denote y^T as the i-th row of $W_1 \in \mathbb{R}^{n_1 \times n_0}$. Then, the activation input $\nu_1 = W_1\omega^0 + b_1$ is bounded below and above by $\underline{\nu}_1$ and $\overline{\nu}_1$, respectively, where the i-th entry of the vectors $\underline{\nu}_1$ and $\overline{\nu}_1$ are given by $\underline{\nu}_{1i} = y^T\overline{n} + b_{1i} - \sum_{i=1}^{n_0} |y_i\underline{n}_i|$ and $\overline{\nu}_{1i} = y^T\overline{n} + b_{1i} + \sum_{i=1}^{n_0} |y_i\underline{n}_i|$, respectively. The sector bounds for the hyperbolic tangent function (see [6] for more details) are $r_1 = 1$ and

$$m_1 = \min\left(\frac{\tanh(\overline{\nu}_1) - \tanh(\nu_1^*)}{\overline{\nu_1} - \nu_1^*}, \frac{\tanh(\nu_1^*) - \tanh(\underline{\nu}_1)}{\nu_1^* - \underline{\nu}_1}\right).$$

Since the activation functions in ϕ_1 are monotonically non-decreasing, then the activation output ω_1 is bounded below by $\underline{\omega}_1 = \phi(\underline{\nu}_1)$ and above by $\overline{\omega}_1 = \phi(\overline{\nu}_1)$. These values can then be used to compute the bounds of the activation input ν_2 of the next layer. Propagating this process through all layers of the NN we obtain the bounds $\underline{\nu} \in \mathbb{R}^{n_\phi}$, and $\overline{\nu} \in \mathbb{R}^{n_\phi}$. Considering these arguments we have the following result:

Lemma 4.1: Let $Z = \{\zeta \in \mathbb{R}^{n_G} : \underline{\zeta} \leq \zeta \leq \overline{\zeta}\}$ be the smallest hypercube that bounds the states. Additionally, consider that the activation functions of the NN defined in (13)-(14) are given by the hyperbolic tangent function. Then, there exist vectors a_ϕ and b_ϕ such that the nonlinearity ϕ defined in (12) satisfies the local sector constraint (16).

E. Lyapunov condition

The stability result of system (7) under the NN controller (13)-(14) is assessed by the following theorem.

Theorem 4.1: Consider the system (7) with the NN controller (13)-(14) with equilibrium point $\zeta^* = 0$ and the state constraint set Z. Let $\underline{\xi}$, $\overline{\xi}$, a_ϕ and b_ϕ be given vectors satisfying Lemma 4.1. Define

$$R_V = \begin{pmatrix} I_{n_G} & 0 \\ N_{ux} & N_{uw} \end{pmatrix}, R_\phi = \begin{pmatrix} N_{vx} & N_{vw} \\ 0 & I_{n_\phi} \end{pmatrix}.$$

If there exist a positive definite matrix $P \in \mathbb{R}^{n_G \times n_G}$ and vector $\theta \in \mathbb{R}^{n_\phi}$ with $\theta \geq 0$ such that $\Theta = \text{diag}(\theta)$ satisfying

$$R_V^T V_1 R_V + R_\phi^T V_2 R_\phi < 0, \tag{18}$$

with

$$V_1 = \begin{pmatrix} A_G^T P A_G - P & A_G^T P B_G \\ B_G^T P A_G & B_G^T P B_G \end{pmatrix},$$

$$V_2 = \begin{pmatrix} -2M_\phi R_\phi \Theta & (M_\phi + R_\phi)\Theta \\ (R_\phi + M_\phi)\Theta & -2\Theta \end{pmatrix},$$

Then the origin of the system (7) with the NN controller (13)-(14) is asymptotically stable.

Proof: Define the Lyapunov function $V(\xi) = \xi^T P \xi$, where $P \in \mathbb{R}^{n_G \times n_G}$ is a positive definite matrix. Then, using (7) we can show that

$$V(\xi(k+1)) - V(\xi(k)) = \begin{pmatrix} \xi(k) \\ w(k) \end{pmatrix}^T R_v^T V_1 R_v \begin{pmatrix} \xi(k) \\ w(k) \end{pmatrix}.$$

Now, from (17) and Lemma 4.1 the following inequality holds:

$$\begin{pmatrix} \xi(k) \\ w(k) \end{pmatrix}^T R_\phi^T V_2 R_\phi \begin{pmatrix} \xi(k) \\ w(k) \end{pmatrix} \leq 0$$

In order to guarantee that the above inequalities are simultaneously satisfied we apply the S-procedure. Thus, if there exists $\Theta = \text{diag}(\theta)$ where $\theta \geq 0$ and if (18) is satisfied it follows that there exists $\epsilon > 0$ such that

$$V(\xi(k+1)) - V(\xi(k)) + \begin{pmatrix} \xi(k) \\ w(k) \end{pmatrix}^T R_\phi^T V_2 R_\phi \begin{pmatrix} \xi(k) \\ w(k) \end{pmatrix} < -\epsilon \|\xi(k)\|^2. \quad (19)$$

Assume that $\xi(k) \in Z$ for some $k \in \mathbb{N}$. Then, the last term on the left-hand side of (19) is greater or equal than zero, and thus the inequality $V(\xi(k+1)) \leq 1$ must hold, which means that $\xi(k+1) \in Z$. Using this idea, we can show by an induction argument that $\xi(0) \in Z$ implies that $x(k) \in Z$ $\forall k \in \mathbb{N}$. Consequently, if $\xi(0) \in \mathcal{E}$ the final term on the left side of (19) is greater or equal to zero $\forall k \in \mathbb{N}$, which means that $V(\xi(k+1)) - V(\xi(k)) \leq -\epsilon \|\xi(k)\|^2$ $\forall k \in \mathbb{N}$. Then, using a standard argument from Lyapunov theory, it follows that the origin of the system (7) with the NN controller (13)-(14) is locally asymptotically stable. ■

V. SIMULATION RESULTS

In this section, we present numerical experiments of the approach proposed in this paper. In the numerical experiments, the model (1)-(5) is considered as virtual plant coded in Matlab with an Euler scheme in time and space, such that $\Delta t = 0.01$ ms and $\Delta z = 0.02$ m, and the Deep Learning Toolbox was used for training the NNs. The values of the model parameters were borrowed from [3] and correspond to a real experimental setup available for the authors. The initial condition of (1)-(5) is given by

$$\alpha_{1,0}(z) = \overline{\alpha}_1 \sin(2z), \quad \alpha_{2,0}(z) = \overline{\alpha}_2 \cos(2z),$$
$$\beta_{1,0}(z) = \overline{\beta}_1 \mathrm{e}^z, \quad \beta_{2,0}(z) = \overline{\beta}_2 (\sin(5z) - 2\cos(z)),$$
$$Q_0 = \overline{Q},$$

where, for $i \in \{1, 2\}$, $\overline{\alpha}_i$, $\overline{\beta}_i$ and $\overline{Q}$ are randomly chosen values (from the standard normal distribution) for generation of training and validation data for the NN controller.

Finally, all simulations were performed on a Intel core i5 8th generation personal computer with 8GB of RAM and 8Mb of memory cache.

1) *Varying the number of hidden layers:* As a first experiment, we consider finding approximations of the NN controllers with a varying number of layers, for a given input set. Specifically, we consider NNs with n_G inputs, 1 output, and $\ell \in \{1, 2, 4, 6, 8\}$ hidden layers, each having 5 neurons per layer. The number of epochs of the models is 500, which was chosen based on the decrease and stabilization of the root mean square error (RMSE) between the output of the NN controller and the backstepping control law (6). For generating the training data, we compute u_{bks} at 62550 time steps, where 10% is used for validation and 90% of the data is used for training the NN by minimizing the mean-squared loss.

TABLE I: Comparison of the NN controller performance for different numbers of layers.

ℓ	Training time [s]	RMSE	σ	$P_{\lambda_{min}}$	$P_{\lambda_{max}}$
1	1447.30	5.98×10^{-2}	11.09	0.78	3.39
2	1732.36	5.37×10^{-2}	10.34	0.84	4.61
4	2163.00	1.91×10^{-2}	9.85	0.64	0.7
6	2908.89	1.87×10^{-2}	9.42	0.46	0.87
8	3852.05	8.6×10^{-3}	8.76	0.74	0.83

The RMSE performance index and the training time of the NN controllers are sumarized in Table I, where σ stands for the standard deviation, and $P_{\lambda_{min}}$ and $P_{\lambda_{max}}$ are the minimum and maximum eigenvalues of matrix P computed through the LMI in (18). As can be seen in Table I, for more then 4 layers the training time increases significantly and the improvement in the RMSE and σ are small. In all cases it was possible to find a positive definite matrix P ensuring the asymptotic stability of the NN controller.

The performance of the backstepping and NN controllers (with $\ell = 4$) is depicted in Figure 1. In Figures 1a-1b, it can be seen that the states are stabilized to the zero equilibrium point by the backstepping and NN controller, respectively. As can be seen in Figure 1d, the NN controller was capable of reproducing a similar transient behavior to backstepping at the same time that the closed-loop system is stabilized.

2) *Uncertain parameters of the system:* In the previous studies, we assume perfect knowledge of the Rijke tube model. In practice, however, it is hard to determine some model parameters such as the steady-state values of the states, the empirical constant of the King's law, the heat release time constant, and reflection losses. Therefore, it is of practical interest to verify the performance of the controller under an uncertain scenario. Here, we investigate the performance of the NN and backstepping controllers given an inaccurate model. The uncertain parameter chosen is c_2 since several of the aforementioned uncertainties enter continuously in this term.

In this scenario the NN controller is trained in a stochastic environment where c_2 is randomly chosen from a uniform distribution of the values $\{1.19, 3.25, 7.5\}$ in each episode. Then the NN controller is validated for each specific scenario. We define $c_2^* = 4.22$ as the nominal value for the backstepping control design while the virtual plant operates with c_2 randomly chosen between $\{1.19, 3.25, 7.5\}$.

Figures 2 shows the mean value of the norm evaluated along the simulated time of both controllers for 20 experiments with random values of c_2 and initial conditions in the

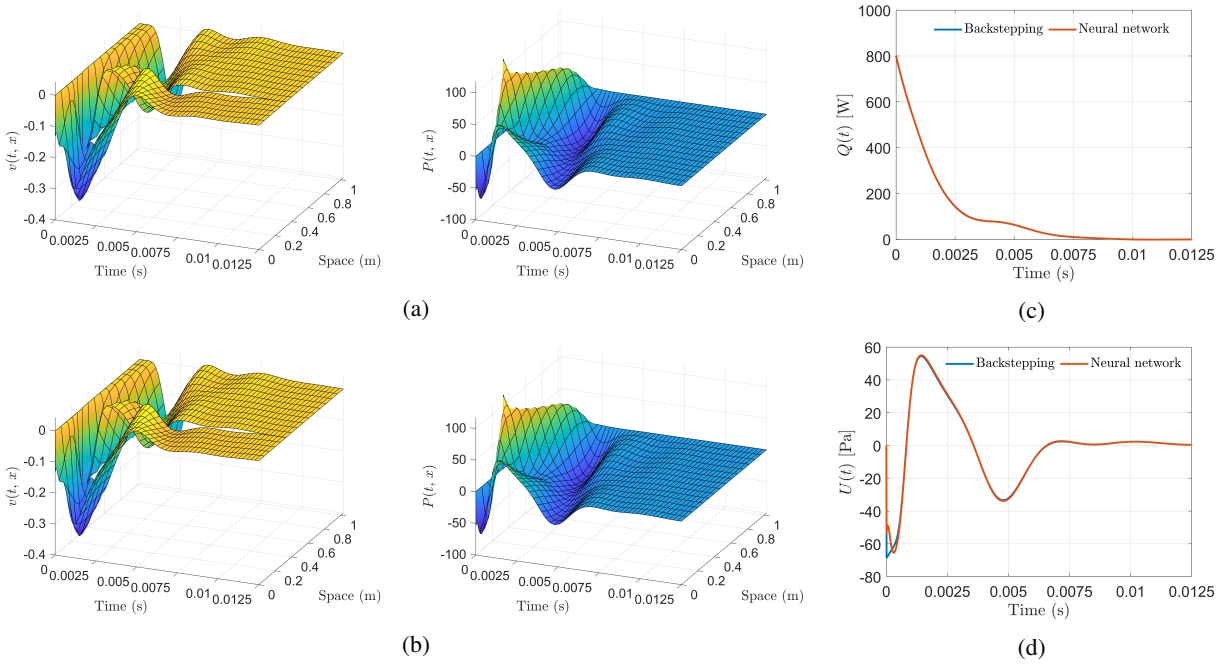

Fig. 1: Velocity, pressure and heat power evolution, and control inputs of the Rijke tube system with the full-state backstepping and NN controller with $\ell = 4$. (a) Velocity and pressure evolution with backstepping controller. (b) Velocity and pressure evolution with neural network controller. (c) Heat power evolution with backstepping and neural network controller. (d) Backstepping and neural network control inputs.

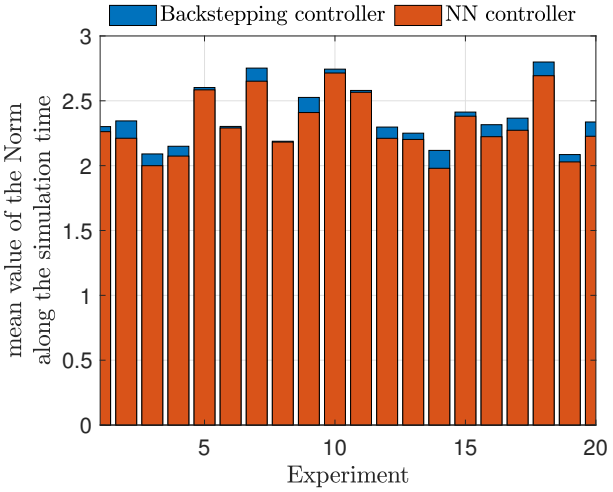

Fig. 2: Mean value of the norm evaluated along the simulated time of the closed-loop system with the backstepping and NN controler in Scenario 2.

distribution data. Comparing the values both controllers in Figure 2, it can be seen that the NN controller has a better performance.

VI. CONCLUSIONS

This paper has introduced a systematic approach for designing NN controllers by imitating the behavior of the full-state backstepping method. Simulations results show that the NN controllers can achieve a similar behavior with the backstepping design in a scenario with perfect knowledge of the model parameters. Future works include real experiments in a setup available to the authors. Other directions are to compare the proposed methodology with adaptive control approaches with robustness guarantees and to analyze the closed-loop stability directly on the PDE instead of finite dimensional approximations.

REFERENCES

[1] A. M. Annaswamy and A. F. Ghoniem. Active control of combustion instability: Theory and practice. *IEEE Control Systems Magazine*, 22:37–54, 2002.

[2] J. Auriol, F. B. Argomedo, and F. Di Meglio. Robustification of stabilizing controllers for ODE-PDE-ODE systems: A filtering approach. *Automatica*, 147:10724, 2023.

[3] G. A. de Andrade, R. Vazquez, and D. J. Pagano. Backstepping stabilization of a linearized ODE-PDE Rijke tube model. *Automatica*, 96:98–109, 2018.

[4] J. P. Epperlein, B. Bamieh, and K. J. Astrom. Thermoacoustics and the Rijke tube: Experiments, identification, and modeling. *IEEE Control Systems Magazine*, 35(2):57–77, 2015.

[5] P. L. Rijke. Notice of a new method of causing a vibration of the air contained in a tube open at both ends. *Philosophical Magazine 4*, 17(116):419–422, 1859.

[6] H. Yin, P. Seiler, M. Jin, and M. Arcak. Imitation learning with stability and safety guarantees. *IEEE Control Systems Letters*, 6:409 – 414, 2021.

[7] U. Zalluhoglu, A. S. Kammer, and N. Olgac. Delayed feedback control laws for Rijke tube thermoacoustic instability, synthesis, and experimental validation. *IEEE Transactions on Control Systems Technology*, 24(5):1861 – 1868, 2016.

[8] D. Zhao, Z. Lu, H. Zhao, X. Y. Li, B. Wang, and P. Liu. A review of active control approaches in stabilizing combustion systems in aerospace industry. *Progress in Aerospace Sciences*, 97:35–60, 2018.